Hunting Axions Using Astrophysical Observation and Quantum Metrology

Yifan Chen

ITP-CAS

27 September 2021,
Very Light Dark Matter 2021, online

Outlines

Motivation and Introduction to Axion

Hunting Axions with Event Horizon Telescope Polarimetric Measurements

Axion Haloscope Array With $\mathcal{PT}$ Symmetry

Motivation and Introduction to Axion

Axion/Axion-like Particle

- Hypothetical pseudoscalar initially motivated by strong CP problem: **Neutron electric dipole** $|\bar{\theta}| 10^{-16}$ **e.cm is smaller than** 10^{-26} **e.cm.**

  $$\bar{\theta} = \theta_{\mathrm{QCD}} + \arg \det M_u M_d, \qquad \text{Fine tuning!}$$

  Why is $\bar{\theta}$ so small? Why instead of ?
  Solution: introducing an **dynamical** field with effective potential

  $$V \sim -m_\Phi^2 f_\Phi^2 \cos(\bar{\theta} + \frac{\Phi}{f_\Phi}).$$

  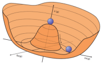

- Extra dimension predicts a wide range of axion mass.
  Dimensional reduction from higher form fields:
  e.g. $A^M(5D) \to A^\mu(4D) + \Phi(4D)$.

- Cold dark matter candidate behaving like **coherent wave**:

  $$\Phi(x^\mu) \simeq \Phi_0(\mathbf{x}) \cos \omega t; \qquad \Phi_0 \simeq \frac{\sqrt{\rho}}{m_\Phi}; \qquad \omega \simeq m_\Phi.$$

  Amplifications of the signals:
  Tabletop experiments on earth: $\rho_{\mathrm{DM}} \sim 0.4$ GeV/cm^3;
  Astrophysical: **larger** ρ, e.g., GC or near Kerr black hole.

Hunting Axions with Event Horizon Telescope Polarimetric Measurements

based on
arxiv: 1905.02213, Phys. Rev. Lett. **124** (2020) no.6, 061102,
arxiv: 2105.04572,
arxiv: 2110.XXXXX,

YC, Chunlong Li, Yuxin Liu, Ru-Sen Lu, Yosuke Mizuno, Jing Shu, Xiao Xue, Qiang Yuan, Yue Zhao, Zihan Zhou

Superradiance and Gravitational Atom

- **Rotational and dissipational medium** can amplify the wave around. [Zeldovichi 72']

- **Superradiance**: the wave-function is exponentially amplified from extracting BH rotation energy when $\lambda_c \simeq r_g$. [Penrose, Starobinsky, Damour et al]

- **Gravitational bound state** between BH and axion cloud:

$$\Phi(x^\mu) = e^{-i\omega t} e^{im\phi} S_{lm}(\theta) R_{lm}(r).$$

- Most efficient for $(l, m) = (1, 1)$ state where $S_{11} \simeq Y_{11} \propto \sin\theta$.

- **Self interaction saturating** phase: $\Phi_{\max} \simeq f_\Phi$. [Yoshino, Kodama 12', Baryakht et al 20']

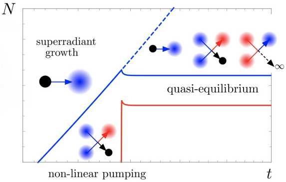

Axion QED: Birefringence

$$\mathcal{L} = -\frac{1}{4}F_{\mu\nu}F^{\mu\nu} - \frac{1}{2}g_{\Phi\gamma}\Phi F_{\mu\nu}\tilde{F}^{\mu\nu} + \frac{1}{2}\partial^{\mu}\Phi\partial_{\mu}\Phi - V(\Phi),$$

- Equation of motion for photon under axion background:

$$[\partial_t^2 - \nabla^2]A_{L,R} = \mp\, 2g_{\Phi\gamma}n^{\mu}\partial_{\mu}\Phi k A_{L,R}.$$

- **Birefringent effect with different dispersion relations**:

$$\omega_{L,R} \sim k \mp g_{\Phi\gamma}n^{\mu}\partial_{\mu}\Phi.$$

- The **electric vector position angle** of linear polarization is shifted by

$$\begin{aligned}\Delta\chi &= g_{\Phi\gamma}\int_{\mathrm{emit}}^{\mathrm{obs}} n^{\mu}\partial_{\mu}\Phi \; dl \\ &= g_{\Phi\gamma}[\Phi(t_{\mathrm{obs}}, \mathbf{x}_{\mathrm{obs}}) - \Phi(t_{\mathrm{emit}}, \mathbf{x}_{\mathrm{emit}})],\end{aligned}$$

- This only depends on the initial and final background axion field values. $\Phi(t_{\mathrm{emit}}, \mathbf{x}_{\mathrm{emit}}) \sim f_{\Phi}$ from superradiant cloud.

Radiative Transfer with Axion Cloud (IPOLE simulation)

- Radiative transfer in terms of linearly polarized Stokes parameters:

$$\frac{d(Q+i\ U)}{ds} = j_Q + i\ j_U + i\left(\rho_V^{\mathrm{FR}} - 2g_{\Phi\gamma}\frac{d\Phi}{ds}\right)(Q+i\ U).$$

Observable on the sky plane: EVPA $\chi \equiv \arg(Q+i\ U)/2$.

- An almost face-on disk (17° for $M87^\star$):

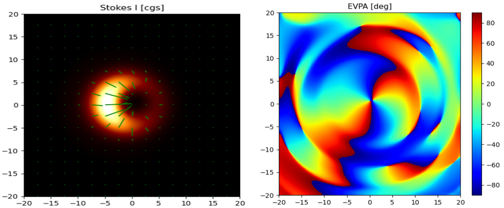

$$\Phi \propto \cos\left[\omega t - \phi\right]\sin\theta \rightarrow \Delta\langle\chi(\varphi)\rangle \propto \mathcal{A}(\varphi)\cos\left[\omega t + \varphi + \delta(\varphi)\right].$$

- **Propagating wave along** φ due to $l=1, m=1$:

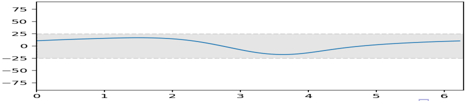

Axion Birefringence Around RIAF (IPOLE simulation)

$$\Delta\langle\chi(\varphi)\rangle = -\mathcal{A}(\varphi)\cos\left[\omega t + \varphi + \delta(\varphi)\right].$$

- Benchmark: **sub-Keplerian RIAF with vertical $\vec{B}$**.

  Axion mass: $\alpha \equiv G_N M_{BH} m_\Phi \in [0.10, 0.44]$ with **period [5, 20] days**.

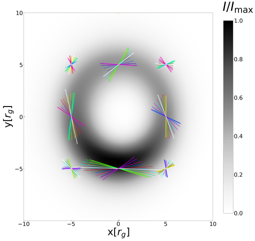

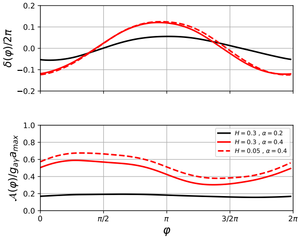

- Phase delay is well fit by $\delta(\varphi) \approx -5\ \alpha\ \sin 17^\circ \cos\varphi$.
- The dominant washout/asymmetry of $\mathcal{A}(\varphi) = \mathcal{O}(1) g_{\Phi\gamma} f_\Phi$ comes from the **lensed photon due to the incoherent phase**!
- For smaller m_Φ, washout is negligible due to longer $\lambda_c \equiv 1/m_\Phi$.

Stringent Constraints on Axion-Photon Coupling

- **Differential EVPA in the time domain**:

$$\langle \chi(\varphi, t_j) \rangle - \langle \chi(\varphi, t_i) \rangle \simeq 2 \sin\left[\omega t_{\rm int}/2\right] \Delta \langle \chi(\varphi) \rangle$$

where $t_{\rm int} \equiv t_j - t_i = 1$ day.

- Uncertainty of azimuthal bin EVPA in EHT data 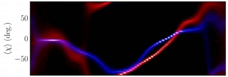

$\rightarrow$ dimensionless **axion photon coupling** $c \equiv 2\pi g_{\Phi\gamma} f_\Phi$.

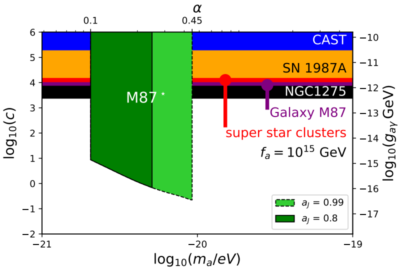

[YC, Liu, Lu, Mizuno, Shu, Xue, Yuan, Zhao 21']

- Weaker bound at small α is due to $R_{11}/R_{\rm max}$ and $\sin\left[\omega t_{\rm int}/2\right]$.

Prospect for next generation EHT

- **Horizon scale SMBH landscape** with ngEHT (space, L2)
  Broader range of axion mass: 10^{-22} eV to 10^{-17} eV.

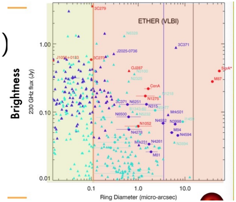

- **Universal birefringence signals** for direct emission only:

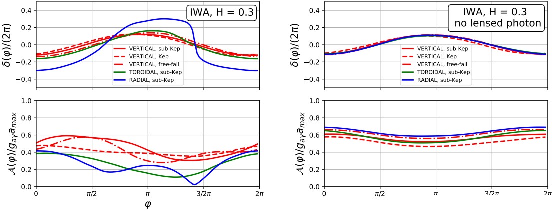

- **Future improvements**:
  Correlation between ΔEVPA at **radius without lensed photon** and different frequency;
  Longer observations;
  Better resolution of EVPA;
  Better understanding of accretion flow and jet.

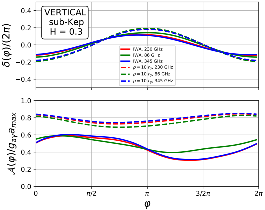

Axion Haloscope Array

With $\mathcal{PT}$ Symmetry

based on
arxiv: 2103.12085

YC, Minyuan Jiang, Yiqiu Ma, Jing Shu and Yuting Yang

Inverse Primakoff and Haloscope [P.Sikivie 83']

$$\nabla \times \mathbf{B} = \partial_t \mathbf{E} + \mathbf{J} - g_{\Phi\gamma} \left(\mathbf{E} \times \nabla\Phi - \mathbf{B}\partial_t\Phi \right).$$

- Inverse Primakoff: $\mathbf{J}_{\text{eff}}(t) = g_{\Phi\gamma}\mathbf{B}\partial_t\Phi$.
- Sikivie cavity Haloscope: $\left(\partial_t^2 + \gamma\partial_t + \omega^2\right)\mathbf{E}_{\text{c}} = \partial_t\mathbf{J}_{\text{eff}}(t)$.
- Static B_0 and resonant when $\omega = m_\Phi \sim V^{-1/3} \sim \mathcal{O}(1)$ GHz.

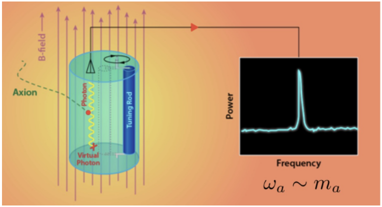

e.g. ADMX, HAYSTACK

Resonant Detection for Lower m_Φ

- Resonant LC circuit [P.Sikivie et al 14']: $m_\Phi = \omega_{\rm LC} = \frac{1}{\sqrt{LC}}$.

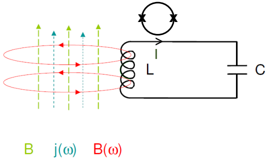

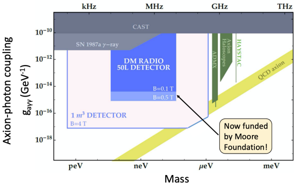

Assumptions: T=10 mK, Q=10^6, 3.5 year integration time, quantum-limited readout

- Resonant SRF Cavity with AC B_0 [Berlin et al 19']

$$\partial_t \mathbf{B}_0 = i\omega_0 \mathbf{B}_0, \quad \omega_1 - \omega_0 = m_\Phi .$$

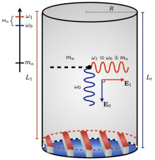

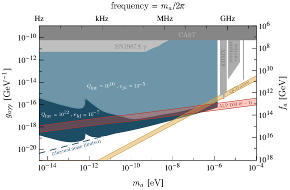

$Q_{\rm int} \equiv \omega/\gamma > 10^{10}$ due to the superconducting nature.

Quantum noise limit for resonant detection

- **Standard quantum limit for power law detection**: [Chaudhuri, Irwin, Graham, Mardon 18']

  resonant intrinsic noise $S_{\rm int}$ + flat readout noise $S_{\rm r}$.

- Sensitivity to $S_{\rm sig}$ and $S_{\rm int}$ is the same.

  SNR^2 $\propto$ range where $S_{\rm int} \gg S_{\rm r}$.

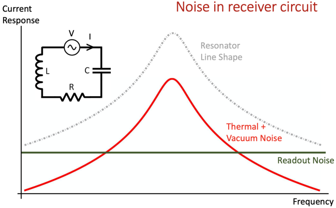

- **Beyond quantum limit**:

  Squeezing $S_{\rm r}$, e.g., HAYSTACK.

  Increasing the sensitivity to $S_{\rm sig}$, e.g., white light cavity in optomechanics/GW detection [Miao, Ma, Zhao, Chen 15'].

White Light Cavity [X.Li, M.Goryachev, Y.Ma et al 20']

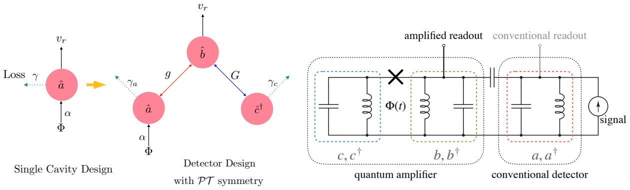

- **Beam-splitting**: $\hbar g(\hat{a}\hat{b}^\dagger + \hat{a}^\dagger \hat{b})$.
- **Non-degenerate parametric amplifier**: $\hbar G(\hat{b}\hat{c} + \hat{b}^\dagger \hat{c}^\dagger)$.

- $\mathcal{PT}$**-symmetry** $(\hat{a} \leftrightarrow \hat{c}^\dagger)$ **emerges** when $g = G$.

$$
\begin{aligned}
(\dot{\hat{a}} + \dot{\hat{c}}^\dagger) &= -i(g-g)\hat{b} - i\alpha\Phi + \cdots ; \\
\dot{\hat{b}} &= -\gamma_r \hat{b} - ig(\hat{a} + \hat{c}^\dagger) + \cdots .
\end{aligned}
$$

- Coherent cancellation leads to **double resonance**. $S_{\rm sig}$ is largely enhanced when $g \gg$ **intrinsic dissipation** γ:

$$
S_{\rm sig}^{\rm WLC}(\Omega) = \frac{2\gamma_r \alpha^2 S_\Phi(\Omega)}{(\gamma + \gamma_r)^2 + \Omega^2} \left(\frac{g^2}{\gamma^2 + \Omega^2} \right).
$$

Resonator Chain Haloscope

- Generalization to chain detector:

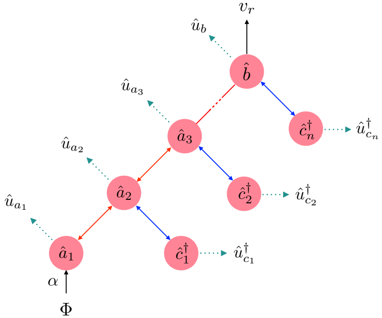

- $\mathcal{PT}$-invariant mode: $\hat{A}_i \equiv \hat{a}_i + \hat{c}_i^\dagger$.

$$\dot{\hat{A}}_1 = -i\alpha\Phi + \cdots\,,$$
$$\dot{\hat{A}}_i = -ig\hat{A}_{i-1} + \cdots\,,$$
$$\dot{\hat{b}} = -\gamma_r\hat{b} - ig\hat{A}_n.$$

$n+1$-times resonance!

- The whole Hamiltonian is explitly $\mathcal{PT}$ **broken**.

- $S_{\rm sig}$ is n-times enhanced:

$$S_{\rm sig}^{\rm RC}(\Omega) = \frac{2\gamma_r\alpha^2 S_\Phi(\Omega)}{(\gamma+\gamma_r)^2+\Omega^2}\left(\frac{g^2}{\gamma^2+\Omega^2}\right)^n.$$

Binary Tree Haloscope

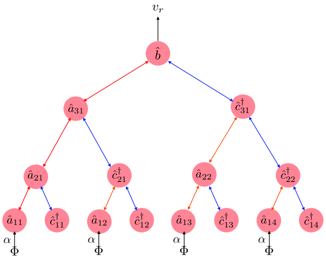

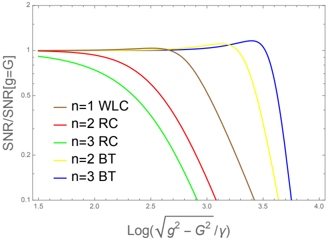

- **Fully $\mathcal{PT}$-symmetric setup** with $\hat{a}_{ij} \leftrightarrow \hat{c}^\dagger_{ij}$ brings strong **robustness**.

- Multi-probing sensors leads to **coherent enhancement**:

$$S^{\mathrm{BT}}_{\mathrm{sig}}(\Omega) = 2^{2n-2} S^{\mathrm{RC}}_{\mathrm{sig}}(\Omega).$$

Signal to Noise Ratio and Physics Reach

- $\mathrm{SNR}^2 \propto$ range where $S_{\mathrm{int}} \gg S_{\mathrm{r}} \propto 2^n \left(\frac{g}{\gamma n_{\mathrm{occ}}}\right)^{\frac{2n}{2n+1}}$.

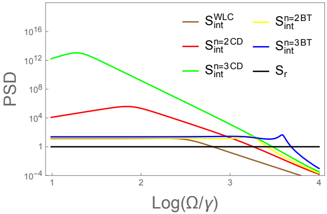

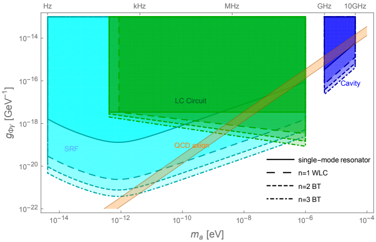

- g/γ can be as large as Q_{int}.
- Large n_{occ} at low frequency for LC circuit makes the enhancement ineffective.
- High Q_{int} and constant n_{occ} for SRF with BT can cover $m_\Phi >$ kHz QCD axion dark matter potentially.

Summary

- Hunting axion cloud with EHT polarimetry:
  Most dense axion field saturating $\Phi \simeq f_\Phi$.

- $\mathcal{PT}$-symmetric array of axion dark matter detectors:
  Multi-resonant systems strongly enhances the sensitivity to signals.

- **Astrophysical observations** and **quantum metrology** can play huge rules in the fundamental physics!

Thank you!

Appendix

Axion Coupling to the Standard Model

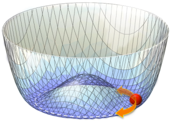

- **Axion Fermion coupling**: $\partial_\mu \Phi \bar{\psi}\gamma^\mu\gamma_5\psi/f_\Phi$,
  non-linearization of a chiral global symmetry $\sim \partial_\mu \Phi J_5^\mu/f_\Phi$.
  Stellar cooling, DM wind/gradient.

- **Axion Gluon coupling**: $\Phi \mathrm{Tr}\, G_{\mu\nu}\tilde{G}^{\mu\nu}/f_\Phi$,
  generated from anomaly/triangle loop diagram.
  Oscillating EDM.

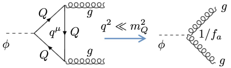

- **Axion Photon coupling**: $\Phi F_{\mu\nu}\tilde{F}^{\mu\nu}/f_\Phi$,
  from mixing with neutral π_0.
  Photon conversion to axion, inverse Primakoff, birefringence.

Axion Field Value

$$\Phi(x^\mu) = e^{-i\omega t} e^{im\phi} S_{lm}(\theta) R_{lm}(r),$$

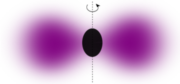

- R_{11} at the **emission point of the ring** can be **near the maximum**, e.g. : whose radius $r_{\max}$ moves farther with smaller $\alpha \equiv G_N M_{BH} m_\Phi \equiv r_g/\lambda_c$.

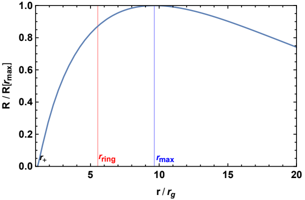

- The wave function **peaks at the equatorial plane of the black hole** since $S_{11} \simeq Y_{11} \propto \sin\theta$.

- **Self interaction saturating phase where $\Phi_{\max} \simeq f_\Phi$.** [Yoshino, Kodama 12', Baryakht et al 20']

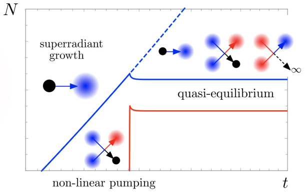

Radiative Transfer and Birefringence

$$\mathcal{L} \ni -\frac{1}{2} g_{\Phi\gamma} \Phi F_{\mu\nu} \tilde{F}^{\mu\nu},$$

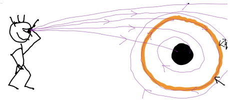

- $\Delta\chi = g_{\Phi\gamma}[\Phi_f - \Phi_i]$ **only applies to point-like source in vacuum**.
- Extended sources, plasma and general relativity effect?

  Radiative transfer in terms of linearly polarized Stokes parameters:

$$\frac{d(Q + i\ U)}{ds} = j_Q + i\ j_U + i \left(\rho_V^{\mathrm{FR}} - 2 g_{\Phi\gamma} \frac{d\Phi}{ds} \right) (Q + i\ U).$$

  ρ_V^{FR}: astrophysical faraday rotation, frequency dependent.

  $2 g_{\Phi\gamma} \frac{d\Phi}{ds}$: **gradient of axion field along geodesics**, achromatic.

  Observable on the sky plane: EVPA $\chi \equiv \arg(Q + i\ U)/2$.

- Since $\Phi \propto \cos\omega t$, **source size** $> \lambda_c \equiv 1/m_\Phi$ can wash out the EVPA oscillation.

EHT Polarization Data Characterization

- Four days' polarization map with slight difference on sequential days:

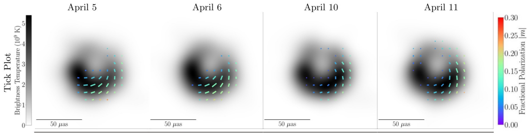

[EHT 2021]

- Uncertainty of the azimuthal bin EVPA from `polsolve`:

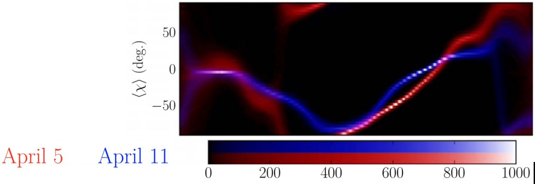

[EHT 2021]

ranging from $\pm 3^\circ$ to $\pm 15^\circ$ for the bins used.

Summary

- **Linearly polarized radiation from dense axion field**:

  Oscillating axion background $\rightarrow$ **EVPA oscillates**.

- **Dissectinng superradiant axion cloud**:

  Superradince brings **large density of axion cloud** carrying angular momentum. $\rightarrow \Delta\mathrm{EVPA}(\varphi)$ is like **a propagating wave along** φ.

- **Stringent Constraints from EHT polarimetric measurements**:

  Using **differential EVPA in time domain**, the uncertainty of azimuthal bin EVPA data on 4 days (2 pairs) can already constrain **axion-photon coupling** to previously unexplored region.

Axion QED: Inverse Primakoff Effect

- Axion-electrodynamics modifies Maxwell equations:

$$\nabla \cdot \mathbf{E} = \rho - g_{\Phi\gamma} \mathbf{B} \cdot \nabla \Phi$$
$$\nabla \times \mathbf{B} = \partial_t \mathbf{E} + \mathbf{J} - g_{\Phi\gamma} \left(\mathbf{E} \times \nabla \Phi - \mathbf{B} \partial_t \Phi \right)$$

- Neglecting spatial derivative, background $\mathbf{B}_0$ and **axion dark matter** Φ leads to **effective current**

$$J_{\rm eff}(t) \sim g_{\Phi\gamma} B_0(t) \sqrt{\rho_{\rm DM}} \cos m_\Phi t.$$

- Inverse Primakoff effect: the conversion of axion to an **oscillating EM field** under background $\mathbf{B}_0$.

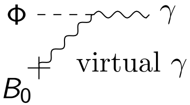

Astrophysical Birefringence from Soliton Core

$$\Delta\Theta_\gamma = g_{a\gamma}[a(t_{\rm obs}, \mathbf{x}_{\rm obs}) - a(t_{\rm emit}, \mathbf{x}_{\rm emit})],$$

- Large initial axion field values in galaxy center: soliton core. **Fuzzy dark matter** [Hu et al 00'], with de Broglie wavelength $\sim$ kpc scale suppressing small scale structures and **a soliton core formed inside GC**.

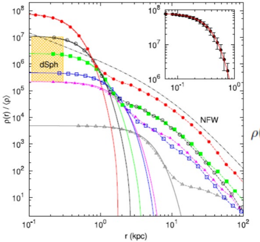

soliton solution

$$\rho(x) = \begin{cases} 0.019\left(\frac{m_a}{m_{a,0}}\right)^{-2}\left(\frac{l_c}{1\mathrm{kpc}}\right)^{-4} M_\odot \mathrm{pc}^{-3}, & \text{for } r < l_c \\ \frac{\rho_0}{r/R_H(1+r/R_H)^2}, & \text{for } r > l_c \end{cases}$$

NFW profile

[Schive et al 14']

Balance between quantum pressure and gravitational self interaction.

Birefringence from Soliton Core Axion

- Ultralight axion dark matter forms soliton core in the galaxy center.

$$\Delta\chi = g_{\Phi\gamma}[\Phi(t_{\rm obs}, \mathbf{x}_{\rm obs}) - \Phi(t_{\rm emit}, \mathbf{x}_{\rm emit})],$$

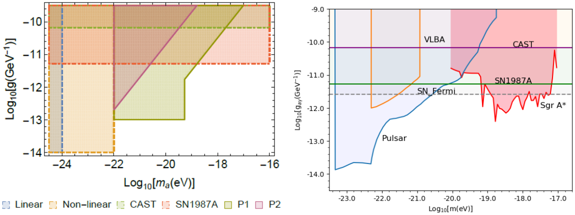

- Linearly polarized photon from **pulsar**. [Liu, Smoot, Zhao, 19']

- Polarized radiation from **Sgr A***.[Yuan, Xia, YC, Yuan et al 20']

Search Strategies

A region with:

- **Large axion density**
  Outside black hole?
- **Source for linearly polarized photon**
  Stable initial position angle.

Search for:

- **Position angle oscillates with time**;
  Axion is an oscillating background field.
- **Oscillation amplitude change as a function of spatial distribution.**
  Extended light source.

Scenarios: EHT-SMBH
Later we will see to a **radiation ring** instead of a point source is necessary for polarimetric probing of axion.

Event Horizon Telescope: an Earth-sized Telescope

- For single telescope with diameter D, the angular resolution for photon of wavelength λ is around $\frac{\lambda}{D}$;
- VLBI: for multiple radio telescopes, the effective D becomes the maximum separation between the telescopes.

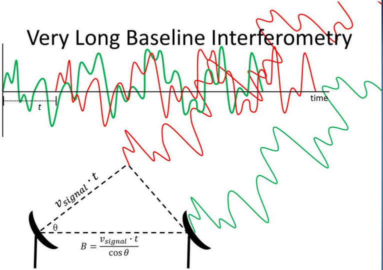

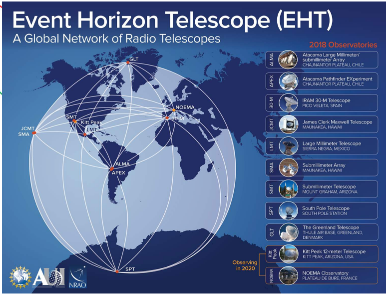

- As good as being able to see  on the moon from the Earth.

Supermassive Black Hole (SMBH) $M87^{\star}$

- To see the **shadow** and the ring, an excellent spatial resolution is necessary.
- One of the most massive black hole ever known: $6.5 \times 10^9 M_{\odot}$;
- Nearly extreme Kerr black hole: $a_J > 0.8$;
- Almost face-on disk with a 17° inclination angle;
- Rich astrophysical information under extremal condition;
- **What else can we learn?**

Fate of Superradiance

Axion cloud can't keep growing exponentially. What's **the fate of it**?

- **Self interaction** of axion becomes important for $f_a < 10^{16}$ GeV. [Yoshino, Kodama 12', Baryakht et al 20']
- Black hole **spins down** until the superradiance condition is violated for $f_a > 10^{16}$ GeV. [Arvanitakia, Dubovsky 10']
- Formation of a **binary system** leads to the decay/transition of the bound state. [Chia et al 18']
- **Electromagnetic blast** for strong (large field value) axion-photon coupling. [Boskovic et al 18']

Weakly Saturating Axion Cloud

- When the field value is large enough, one should take into account the non-perturbative axion potential:

$$V = \mu^2 f^2 \left(1 - \cos\frac{a}{f}\right) = \frac{\mu^2 a^2}{2} - \frac{\mu^2 a^4}{24 f^2} + \ldots;$$

- A quasi periodic phase where **superradiance and non-linear interaction induced emission balance each other** with $\Phi_{\mathbf{peak}} = a_0/f \sim 1$.

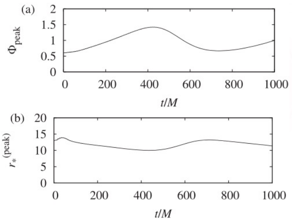

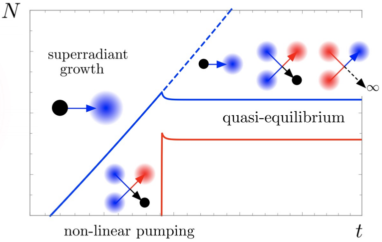

[Yoshino, Kodama 12' 15', Baryakht et al 20']

Black Hole Spin Measurements [Arvanitakia et al 10' 14']

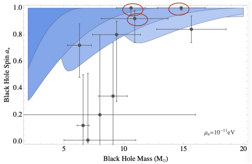

- Comparing **the timescale between the superradiance and BH accretion**, a BH with large spin can typically exclude axion with $f_a > 10^{16}$ GeV.

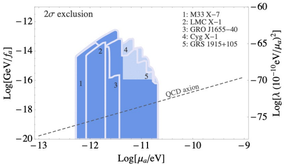

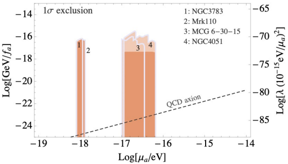

Gravitational Collider [Chia et al 18']

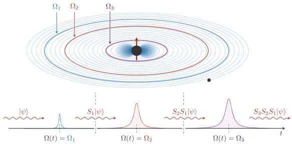

- Resonant transition from one bound state to another happens when orbital frequency Ω **matches the energy gap**.
- Due to the GW emission of the binary system, $\Omega(t)$ slowly increases and scan the spectrum.
- Orbits could float or shrink dependent on the transition.

Detectability of EHT

- Average effect due to the limited resolution and angular dependent phase:

$$\int_0^{\Delta\phi} \cos(\mu t + m\phi) d\phi = \frac{\sin(m\Delta\phi/2)}{m\Delta\phi/2} \cos(\mu t + m\Delta\phi/2).$$

- In the past, we only saw a point instead of a **ring**, $\boldsymbol{\Delta}\phi = \mathbf{2}\pi$, no birefringent effect.

- A subset of the EHT configuration previously measured the position angle at precision of $\sim 3^\circ$. It's reasonable to expect better precision.

Misalignment Production of QCD Axion

- For QCD axion, $m_\Phi f_\Phi \sim \Lambda_{\rm QCD}^2$ predicts a **thin line in the parameter space**.
- Cosmological parameter: initial misalignment angle $\theta_i \equiv \Phi_i / f_\Phi$.

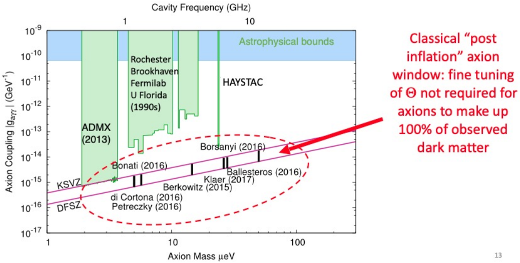

- Assuming $\theta_i \sim 1$ leads to the most natural region of QCD axion dark matter $m_\Phi \sim 10^{-6}\mathrm{eV} \sim$ GHz.
- Different cosmological evolutions can still provide a viable dark matter candidate in other region, e.g., PQ symmetry broken before inflation.

Property of Axion Dark Matter

Galaxy formation: virialization gave $\sim 10^{-3}c$ velocity fluctuation, thus kinetic energy $\sim 10^{-6} m_\Phi c^2$ currently.

Effectively coherent wave:

$$\Phi(\vec{x}, t) = \frac{\sqrt{2\rho_\Phi}}{m_\Phi} \cos\left(\omega_\Phi t - \vec{k}_\Phi \cdot \vec{x} + \delta_0\right).$$

- Bandwidth: $\delta\omega_\Phi \simeq m_\Phi \left\langle v_{\mathrm{DM}}^2 \right\rangle \simeq 10^{-6} m_\Phi$, $Q_\Phi \simeq 10^6$.
- Correlation time: $\tau_\Phi \simeq \mathrm{ms}\,\frac{10^{-6}\mathrm{eV}}{m_\Phi}$.
  Power law detection is used to make integration time longer than τ_Φ.
- Correlation length: $\lambda_d \simeq 200\ \mathrm{m}\frac{10^{-6}\mathrm{eV}}{m_\Phi} \gg \lambda_c = 1/m_\Phi$.
  Sensor array can be used within λ_d.

Higher Frequency Electromagnetic Resonant Detection

Difficult to detect $m_\Phi \gg$ GHz axion dark matter due to short λ_c.

I 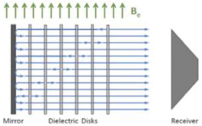

II 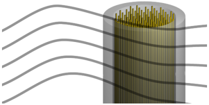

III 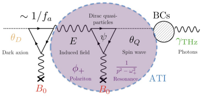

- I **Dielectric Haloscope**: discontinuity of E-field leads to coherent emission of photons from each surface, up to 50 GHz. [A.Caldwell et al 17']

- II **Plasma Haloscope**: using tunable cryogenic plasma to match axion mass, up to 100 GHz. [M.Lawson et al 19']

- III **Topological Insulator**: quasiparticle in it mixing with E field becomes polariton whose frequency can be tuned by magnetic field, up to THz. [D.J.E.Marsh et al 19']

Quantization of Cavity/Circuit Mode

- In Coulomb gauge, vector potential can be quantized

$$\vec{A}_k(\vec{r}, t) = \sum_k \left(\frac{1}{2\omega_k}\right)^{1/2} \hat{a}_k u_k(\vec{r}) e^{-i\omega_k t} + h.c..$$

where $u_k(\vec{r})$ form a complete orthonormal set for a given boundary condition and $[\hat{a}_k, \hat{a}_{k'}] = \delta_{kk'}$.

- The Hamiltonian for each mode reduces to harmonic oscillator

$$H_{\mathrm{cavity}} = \frac{1}{2}\int \left(\vec{E}^2 + \vec{B}^2\right) d^3\vec{x} = \sum_k \omega_k \left(\hat{a}_k^\dagger \hat{a}_k + \frac{1}{2}\right).$$

- In the interaction picture, the coupling to axion is

$$H_{\mathrm{int}} = \int g_{\Phi\gamma} \Phi \vec{E} \cdot \vec{B}_0 d^3\vec{x} = \alpha \Phi(\hat{a} + \hat{a}^\dagger), \quad \alpha \simeq g_{\Phi\gamma} B_0 \sqrt{m_\Phi V}.$$

- Circuit mode can be quantized in the same way

$$H_{\mathrm{LC}} = \frac{\hat{Q}^2}{2C} + \frac{\hat{\phi}^2}{2L} = \omega_{\mathrm{LC}} \left(\hat{a}^\dagger \hat{a} + \frac{1}{2}\right).$$

Open quantum system

A quantum-mechanical system interacting with the environment:

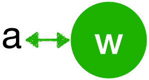

- System mode $\hat{a}$ couples to infinite degrees of freedom $\hat{w}_\omega$:

$$i\hbar\sqrt{2\gamma_r}\int_{-\infty}^{+\infty}\frac{d\omega}{2\pi}[\hat{a}^\dagger\hat{w}_\omega - \hat{a}\hat{w}_\omega^\dagger] + \int_{-\infty}^{+\infty}\frac{d\omega}{2\pi}\hbar\omega\hat{w}_\omega^\dagger\hat{w}_\omega.$$

- Fourier transformation: **0-dim localized mode** $\hat{a}$ couples to an 1-dim bulk w_ξ (transmission line):

$$i\hbar\sqrt{2\gamma_r}\hat{a}^\dagger\hat{w}_{\xi=0} + \mathrm{h.c.} + i\hbar\int_{-\infty}^{+\infty}d\xi\,\hat{w}_\xi^\dagger\partial_\xi\hat{w}_\xi.$$

- Equations of motion for $\hat{a}$ and outgoing mode $\hat{w}_{0_+}$:

$$\dot{\hat{a}} = -\gamma_r\hat{a} + \sqrt{2\gamma_r}\hat{w}_{0_-}; \qquad \hat{w}_{0_+} = \hat{w}_{0_-} - \sqrt{2\gamma_r}\hat{a}$$

Single Mode Resonator as Quantum Sensor

- For a resonator $\hat{a}$ **probing weak signal** Φ: $\alpha\left(\hat{a}+\hat{a}^{\dagger}\right)\Phi$
- Readout for outgoing mode $\hat{v}_r \equiv \hat{w}_{0_+}$:

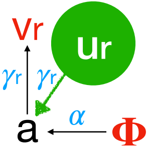

$$\hat{v}_r = \frac{\Omega - i\gamma_r}{\Omega + i\gamma_r}\hat{u}_r + \frac{\sqrt{2\gamma_r}\alpha}{\Omega + i\gamma_r}\Phi.$$

- Vacuum fluctuation in incoming mode $\hat{u}_r \equiv \hat{w}_{0_-}$ with white noise power spectral density $S_{\mathrm{r}} = 1$.
- Resonant signal spectrum $S_{\mathrm{sig}} = \frac{2\gamma_r\alpha^2}{\gamma_r^2+\Omega^2}\ S_\Phi(\Omega)$.

$$\text{Scan rate: } \int_{-\infty}^{+\infty} \frac{2\gamma_r\alpha^2}{\gamma_r^2 + \Omega^2} d\Omega = \frac{\alpha^2}{2\pi}.$$

- Trade-off between peak sensitivity and bandwidth by tuning γ_r.

Intrinsic loss and fluctuation

- However, **intrinsic loss** proportional to γ exists, characterized by the quality factor $Q_{\rm int} \equiv \omega/\gamma$.

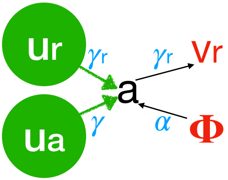

- According to the **fluctuation-dissipation theorem**, there is intrinsic noise $S_{\rm int}(\Omega) = \frac{4\gamma\gamma_r}{(\gamma+\gamma_r)^2+\Omega^2} S_{u_a}$ whose PSD contains both vacuum and thermal fluctuations:

$$S_{u_a} = n_{\rm occ} \equiv \left(\frac{1}{2} + \frac{1}{\exp(\omega/T) - 1}\right) \simeq \begin{cases} \frac{1}{2} & T \ll \omega; \\ \frac{T}{\omega} & T \gg \omega. \end{cases}$$

- **Standard quantum limit for power law detection:** **resonant $S_{\rm int}$+ flat $S_{\rm r}$**. [Chaudhuri et al 18']

Beam splitting coupling

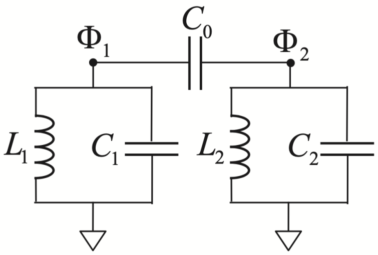

- Use an additional capacitor to couple two LC circuits:

$$H = \frac{1}{2}C_1\dot{\phi}_1^2 + \frac{1}{2}C_2\dot{\phi}_2^2 + \frac{1}{2L_1}\phi_1^2 + \frac{1}{2L_2}\phi_2^2 + \frac{1}{2}C_0(\dot{\phi}_1 - \dot{\phi}_2)^2.$$

- Conjugate momentum to ϕ_i involves mixing. Interaction potential:

$$\beta\hbar\sqrt{\omega_1\omega_2}(\hat{a}_1 - \hat{a}_1^\dagger)(\hat{a}_2 - \hat{a}_2^\dagger) \sim \hat{a}_1\hat{a}_2^\dagger + h.c.,$$

Non-Degenerate Parametric amplifier coupling

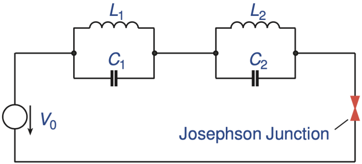

- Use a DC voltage and a Josephson junction to couple two LC circuits:

$$
\begin{aligned}
V &= -\frac{\hbar I_J}{2e_0}\cos\left(\omega_0 t + \frac{2e_0}{\hbar}(\phi_2+\phi_3)\right) \\
&= -\frac{\hbar I_J}{2e_0}\cos\left(\omega_0 t + \kappa_2(a_2+a_2^\dagger)+\kappa_3(a_3+a_3^\dagger)\right) \\
&\sim \frac{\hbar I_J}{4e_0}\kappa_2\kappa_3[a_2 a_3 + a_2^\dagger a_3^\dagger],
\end{aligned}
$$

Kinetic Mixing Dark Photon Dark Matter

- An additional $U(1)$ vector can have kinetic mixing with electromagnetic photon field through
$$\varepsilon F_{\mu\nu} F'^{\mu\nu}.$$
- It appears generally in theory with extra-dimension with a broad mass window predicted.
- Cold dark matter candidate behaving like **coherent wave**:

From Axion QED to Kinetic Mixing Dark Photon

$$\nabla \times \mathbf{B} = \partial_t \mathbf{E} + \mathbf{J} - g_{\Phi\gamma} \left(\mathbf{E} \times \nabla\Phi - \mathbf{B}\partial_t\Phi \right)$$

- Axion dark matter leads to an effective current under background $\mathbf{B}_0$ with $|J_{\rm eff}(t)| \sim g_{\Phi\gamma} B_0(t) \sqrt{\rho_{\rm DM}} \cos m_\Phi t$.

$$-\frac{1}{4}\left(\tilde{F}_{\mu\nu}\tilde{F}^{\mu\nu} + \tilde{F}'_{\mu\nu}\tilde{F}'^{\mu\nu}\right) + \frac{1}{2} m_{\gamma'}^2 \tilde{A}'_\mu \tilde{A}'^\mu - eJ^\mu_{\rm EM}\tilde{A}_\mu + \varepsilon m_{\gamma'}^2 \tilde{A}_\mu \tilde{A}'^\mu .$$

- Similarly, in the interaction basis, the background dark photon behaves as an effective electromagnetic current with $J^\mu_{\rm eff} = \varepsilon m_{\gamma'}^2 \tilde{A}'^\mu$.

Effective current induced magnetic field

- In a space screened by electromagnetic shielding, the effective current can induce a transverse magnetic field
- For axion:

$$B_a \approx |\vec{J}_a^{\rm eff}| \; V^{1/3}, \\ \approx 10^{-17}\mathrm{T}\left(\frac{g_{a\gamma}}{10^{-11}\ \mathrm{GeV}^{-1}}\right)\left(\frac{B_0}{1\ \mathrm{T}}\right)\left(\frac{V^{1/3}}{1\ \mathrm{m}}\right)$$

- For kinetic mixing dark photon (with a factor of 1/3 due to the isotropic wave-funtion):

$$B_{dp} \approx |\vec{J}_{dp}^{\rm eff}| \; V^{1/3}, \\ \approx 10^{-16}\mathrm{T}\left(\frac{\varepsilon}{10^{-6}}\right)\left(\frac{m_{dp}}{10\mathrm{Hz}}\right)\left(\frac{V^{1/3}}{1\ \mathrm{m}}\right).$$

- V is the volume of the EM shielding room. Magnetic field signal is the strongest at the corner of the room.